

This is an Accepted Manuscript for Epidemiology & Infection. Subject to change during the editing and production process.

DOI: 10.1017/S0950268825000214

1 **BAYESIAN SPATIO-TEMPORAL MODELLING OF TUBERCULOSIS IN**

2 **VIETNAM: INSIGHTS FROM A LOCAL-AREA ANALYSIS**

3 **Long Viet Bui^{1,*}, Romain Ragonnet¹, Angus E. Hughes¹, Hoa Binh Nguyen^{2,3}, Nam Hoang Do^{2,3},**
4 **Emma S. McBryde⁴, Justin Sexton^{4,5}, Thuy Phuong Nguyen⁶, David S. Shipman¹, Greg J. Fox^{7,8},**
5 **James M. Trauer¹**

6 **¹ School of Public Health and Preventive Medicine, Monash University, Melbourne, Victoria,**
7 **Australia**

8 **² National Tuberculosis Program, Ha Noi, Viet Nam**

9 **³ National Lung Hospital, Ha Noi, Viet Nam**

10 **⁴ Australian Institute of Tropical Health & Medicine, James Cook University, Townsville,**
11 **Queensland, Australia**

12 **⁵ Commonwealth Scientific and Industrial Research Organisation (CSIRO), Australia**

13 **⁶ Sydney Medical School, University of Sydney, Sydney, New South Wales, Australia**

14 **⁷ Faculty of Medicine and Health, The University of Sydney, Sydney, New South Wales, Australia**

15 **⁸ The Woolcock Institute for Medical Research, Glebe, New South Wales, Australia**

16 *** Corresponding author, email viet.bui1@monash.edu**

17

This is an Open Access article, distributed under the terms of the Creative Commons Attribution-NonCommercial-NoDerivatives licence (<http://creativecommons.org/licenses/by-nc-nd/4.0/>), which permits non-commercial re-use, distribution, and reproduction in any medium, provided the original work is unaltered and is properly cited. The written permission of Cambridge University Press must be obtained for commercial re-use or in order to create a derivative work.

18 **SUMMARY**

19 Spatial analysis and disease mapping have the potential to enhance understanding of tuberculosis
20 (TB) dynamics, whose spatial dynamics may be complicated by the mix of short and long range of
21 transmission and long latency period. TB notifications in Nam Dinh Province for individuals aged 15
22 and older from 2013 to 2022 were analyzed with a variety of spatio-temporal methods. The study
23 commenced with an analysis of spatial autocorrelation to identify clustering patterns, followed by the
24 evaluation of several candidate Bayesian spatio-temporal models. These models varied from simple
25 assessments of spatial heterogeneity to more complex configurations incorporating covariates and
26 interactions. The findings highlighted a peak in the TB notification rate in 2017, with 98 cases per
27 100,000 population, followed by a sharp decline in 2021. Significant spatial autocorrelation at the
28 commune level was detected over most of the ten-year period. The Bayesian model that best
29 balanced goodness-of-fit and complexity indicated that TB trends associated with poverty: each
30 percentage point increase in the proportion of households that are poor was associated with a 1.3%
31 increase in TB notifications, emphasizing a significant socioeconomic factor in TB transmission
32 dynamics. The integration of local socioeconomic data with spatio-temporal analysis could further
33 enhance our understanding of TB epidemiology.

34 **Keywords:** Tuberculosis, Viet Nam, spatio-temporal analysis, Bayesian modelling, space-time
35 interaction.

36

37

38 INTRODUCTION

39 Despite recent advances, tuberculosis (TB), the infectious disease caused by *Mycobacterium*
40 *tuberculosis* (*M.tb*), continues to pose substantial public health hurdles due to diagnostic challenges,
41 treatment complexities and the emergence of drug-resistant strains [1]. Vietnam, recognised as one of
42 the top 30 countries for TB burden, exemplifies the global struggle against this infectious threat [2].

43 As a directly transmitted infectious disease, TB is linked with several population characteristics that
44 may be spatially correlated, although there is a variable and often lengthy delay between infection and
45 disease onset [3]. As such, people living in high-burden areas might actively spread TB to
46 neighbouring regions [4]. While TB notifications do not directly reflect the true underlying incidence of
47 TB, they still provide valuable information about TB burden and the effectiveness of control measures.
48 Notifications reflect the number of TB cases that have been identified and reported, which can be
49 influenced by the underlying transmission of *M.tb*, as well as factors including novel diagnostic
50 techniques, enhanced detection efforts and the overall treatment outcomes achieved by control
51 programs [5,6].

52 Spatial analysis and disease mapping are powerful methods for understanding infectious diseases
53 such as TB. These techniques can identify high-incidence areas, improve understanding of
54 transmission dynamics, evaluate the impact of public health interventions and investigate
55 socioeconomic risk factors. These insights can support the design of targeted interventions, with the
56 potential to allocate resources more efficiently and reduce the burden of TB [7].

57 Bayesian spatio-temporal analysis methods have gained popularity in disease mapping over recent
58 decades. By incorporating prior knowledge and leveraging data from appropriate neighbouring areas
59 or time points, these methods provide more stable and accurate estimates, even in regions with
60 sparse data. Utilizing these approaches enhances our ability to discern patterns and relationships that
61 might otherwise be obscured, offering the potential for insights into both the current state of the
62 disease and its future course. This can prove invaluable in planning and implementing more effective
63 public health strategies, optimizing intervention timing, and understanding the factors driving disease
64 spread, ultimately leading to more informed decision-making and improved outcomes in TB control
65 [8,9].

66 Bayesian spatio-temporal modelling for diseases has progressed significantly over recent decades,
67 starting from the foundational models of Clayton and Kaldor (1987) and Besag et al. (1991).

68 Bernardinelli et al. (1995) added models with area-specific intercepts and assumed linear temporal
69 trends, while Waller et al. (1997) treated time as exchangeable, using Besag et al.'s hierarchical
70 model independently at each time point without considering temporal risk. Knorr-Held and Besag
71 (1998) merged this spatial model with dynamic, non-parametric models for estimating temporal
72 trends, keeping temporal and spatial effects additive. Knorr-Held (2000) further developed these
73 models, proposing a framework of four types of space-time interactions that explain disease variation
74 beyond simple temporal and spatial effects. These range from unstructured (Type I) to complex
75 structured interactions of space and time (Type IV) [10,11].

76 In this study, we applied Bayesian approaches to investigate the spatial and temporal distribution of
77 routinely notified TB cases during the period 2013 to 2022 and identified potential influencing factors
78 at the local level in a single province in Vietnam.

79 We selected Nam Dinh Province for our analysis because its data is considered reliable by national
80 authorities, and TB notification rates are similar to the national average. Its combination of urban and
81 rural populations, and diverse socio-economic conditions make it a useful case study for
82 understanding *M.tb* transmission dynamics, with findings potentially applicable to the broader national
83 context of Vietnam and beyond.

84

85 **METHODS**

86 **1. Settings:** Nam Dinh Province is located in the southern part of Vietnam's Red River Delta, covers
87 1,676 km² and has a population of approximately 1.83 million. The population is spread over one
88 provincial city, which consists of 22 wards and three communes, and nine rural districts, comprising
89 201 towns/communes. Characterized by flat terrain, the province has higher population densities in
90 the provincial city (Nam Dinh City), reflecting the typical urban concentration of a regional economic
91 and administrative hub.

92 **2. Datasets:** We analysed TB notifications in Nam Dinh Province from 2013 to 2022, considering all
93 forms of TB (new and relapsed cases, both pulmonary and extrapulmonary TB and including non-
94 bacteriologically confirmed cases) occurring in individuals aged 15 and above. Notification data,
95 aggregated at the commune level, was sourced from the Vietnam National TB Programme's
96 database. Additionally, we acquired a dataset at the commune level from the Nam Dinh Statistical
97 Office, detailing the names of communes, population data and proportion of households living below

98 the national poverty standard over the analysis period, henceforward proportion of poor household.
99 Map figures were produced using a base map of Vietnam from the Database of Global Administrative
100 Areas [12], including commune names, administrative codes, and land areas for visualization.

101 **3. Data analysis**

102 **3.1. Utilization of the adjacency matrix:**

103 In spatial analysis, the adjacency matrix, which defines border relationships between areal units, is a
104 commonly used basis for conducting spatial autocorrelation and modelling. To define spatial
105 relationships among areas, we utilized the queen contiguity matrix [13], such that two communes
106 were considered neighbours if they shared at least one vertex. Figure S1 shows the spatial
107 relationships among 226 communes through the queen contiguity matrix.

108 **3.2. Spatial autocorrelation analysis**

109 The expected number of TB cases for each area i in year t , denoted $E_{i,t}$, was calculated using the
110 formula:

$$111 \quad E_{i,t} = P_{i,t} \times \frac{O_t}{P_t}$$

112 where:

- 113 - $P_{i,t}$: denotes the population in area i at year t ,
- 114 - O_t : denotes the total notified TB cases of all communes for year t ,
- 115 - P_t : denotes the total population of all communes for year t ,
- 116 - i indexes spatial patches (communes) from 1 to 226,
- 117 - t indexes study years from 2013 to 2022.

118 The spatial standardized morbidity risk (SMR) for each commune i at year t is calculated as:

$$119 \quad SMR_{i,t} = \frac{O_{i,t}}{E_{i,t}}$$

120 where $O_{i,t}$ denotes the notified TB cases in commune i at year t .

121 The $SMR_{i,t}$ indicates whether a commune has a higher ($SMR_{i,t} > 1$) or lower ($SMR_{i,t} < 1$) risk than
122 would be expected from the whole province at that specific time point.

123 We analysed spatial patterns with the Global Moran's I Statistic [14], which evaluates overall spatial
124 autocorrelation to identify clustering of TB SMRs.

125 Details of the calculations of Moran's I are described in the Supplementary Material.

126 **3.3. Bayesian spatio-temporal modelling**

127 Our Bayesian spatio-temporal models assumed that the number of cases observed in commune i and
128 year t followed a Poisson distribution:

$$129 \quad O_{i,t} \sim \text{Poisson}(E_{i,t}\theta_{i,t})$$

130 Where $E_{i,t}$ is the expected number of cases, and $\theta_{i,t}$ is the SMR of commune i and year t .

131 We considered twelve candidate models, each addressing various aspects of TB dynamics, ranging
132 from basic spatial distributions to complex interactions over both time and space. Each base model,
133 labelled from Model 1a to Model 6a, was replicated with the inclusion of areal covariates, producing
134 corresponding versions Model 1b through Model 6b.

135 **Model 1a** - Besag-York-Mollié (BYM) model: This model integrates both structured and unstructured
136 spatial effects [15]. The structured spatial effect follows the conditional autoregressive (CAR)
137 approach, where the estimate for each commune is influenced by those of neighbouring communes
138 through the queen contiguity matrix introduced above. In contrast, the unstructured spatial effect aims
139 to capture independent random noise across distinct locations. There is no time structure nor time
140 component in this model, meaning that observations from different years are treated as independent
141 data points for each spatial unit, without accounting for temporal correlation or trends.

142 Next, we considered models that included temporal structure. Initial analysis showed that the
143 trend of TB SMR of communes during the study period was not linear, as reflected in the decline in
144 TB notifications in 2021. As a result, we did not pursue models with a linear time trend and instead
145 focused on models incorporating a random walk over time. This statistical method models each time
146 period's estimates as updating the previous period's values, allowing for random but dependent
147 changes over time.

148 **Model 2a:** This model included unstructured spatial effects [15] and a temporal random walk. No
149 spatial dependency between neighbouring communes was assumed.

150 **Model 3a – BYM model with random walk in time:** We retained the spatial framework of the Model
151 1a (the BYM model) while incorporating a random walk to account for time-dependent changes in
152 SMRs [15].

153 Next, we explored several types of space-time interaction models [10,11].

154 **Model 4a – BYM model with temporal random walk and Knorr-Held type I space-time**
155 **interactions:** This model used the BYM model and a temporal random walk, combined with
156 unstructured interactions for both time and space. This allowed the model to capture random

157 fluctuations in TB SMR across different periods and locations, accounting for unstructured variability
158 in both dimensions [10].

159 **Model 5a – BYM model with temporal random walk and Knorr-Held type II space-time**

160 **interactions:** In this model, structured temporal effects interact with unstructured spatial effects. This
161 helps to capture random spatial fluctuations and regular temporal trends in TB SMRs [10].

162 **Model 6a – BYM model with temporal random walk and Knorr-Held type III space-time**

163 **interactions:** This model captures the interaction of unstructured temporal effects with structured
164 spatial effects, enabling it to account for both random temporal fluctuations and organized spatial
165 trends or gradients [10].

166 During the preliminary analysis, we investigated the possibility of Type IV interactions [10] to allow for
167 structured interactions across both space and time. However, due to its high number of parameters
168 and the consequent difficulty in fitting this model, we focused on more manageable models that could
169 consistently capture the key relationships within the data.

170 **Selection of priors:** In Bayesian disease mapping, hyperparameters play an important role in
171 shaping the prior distributions of model parameters. These hyperparameters influence the degree of
172 regularization and the flexibility of the model, guiding parameter estimation based on prior knowledge
173 [16]. For spatial effects, these include precision parameters for structured effects, and for unstructured
174 random noise, which determine the degree of spatial smoothness and variability. For temporal effects,
175 precision parameters in random walk priors control the strength of temporal dependency and the
176 flexibility to capturing trends over time. These hyperparameters guide parameter estimation by
177 incorporating prior knowledge, ensuring accurate modelling of spatiotemporal patterns in disease risk
178 [11,17]. Initially, all proposed models were fitted using a log-gamma distribution as the prior for the
179 hyperparameters governing the effect of the spatial and temporal variables, with a shape parameter of
180 1 and a rate of 0.0005. This choice reflects a weakly informative prior, providing broad flexibility to the
181 model.

182 **Covariate selection:** Given the availability of relevant data, we selected the commune-level
183 population density and proportion of households living below the national poverty line [18] as
184 candidate covariates closely related to crowding and poorly ventilated living conditions. As such, we
185 considered them as independent variables that may each influence *M.tb* transmission. Specifically,
186 population density may affect the likelihood of *M.tb* spreading due to close contact, while poverty may

187 impact access to healthcare and living conditions, both of which may be important to *M.tb*
188 transmission dynamics [19]. Table S1 (Supplementary Material) provides summary statistics for the
189 covariates used in the analysis. The proportion of poor households across communes has a mean of
190 3.50%, with a standard deviation (SD) of 2.80% and an interquartile range (IQR) from 1.44% to
191 5.90%. The average population density was 2.5 thousand people/km², with a SD of 2.50 and an IQR
192 ranging from 0.8 to 1.41 thousand people/km².

193 Details of the Bayesian spatio-temporal modeling are provided in the Supplementary Material.

194 **Model evaluation:** Model performance was evaluated using the mean posterior deviance, Deviance
195 Information Criterion (DIC) [20] and Watanabe-Akaike Information Criterion (WAIC) [21]. While mean
196 posterior deviance specifically assesses the model's fit to the data, lower values of DIC and WAIC
197 signify a model's superior ability to balance goodness-of-fit with complexity, thereby indicating better
198 overall model performance.

199 **Sensitivity analysis:**

200 In the initial analysis, we modelled the counts of TB notifications using a Poisson distribution. While
201 the analysed model accounted for random spatial effects of TB notifications, we also explored a
202 negative binomial distribution to assess the model's sensitivity to the statistical distribution chosen to
203 capture the case count data.

204 To assess the robustness of the best-fitting model, we conducted sensitivity analyses by testing
205 alternative sets of hyperparameters for the log-gamma distribution. Specifically, we used a shape
206 parameter of 0.01 with a rate of 0.01, representing a highly diffuse prior, and a shape parameter of 2
207 with a rate of 0.5, reflecting a more concentrated prior. These variations allowed us to evaluate how
208 sensitive the model results were to changes in our prior assumptions. Figure S2 (Supplementary
209 Material) shows the distribution of log-gamma distribution with different values of shape and rate.

210 **3.3. Software:** We used R 4.3.3 [22] for data analysis and visualization. R-INLA [17] was used for
211 spatio-temporal modelling.

212

213 RESULTS

214 From 2013 to 2022, Nam Dinh Province reported a total of 14,887 TB cases in individuals aged over
215 15. Throughout this period, TB notification rates per 100,000 population fluctuated significantly,

216 peaking in 2017 at approximately 98 cases per 100,000 population. By contrast, 2021 recorded the
217 lowest rate at around 60 cases per 100,000 population. Figure 2 illustrates the notification rates from
218 2013 to 2022, while Figure S3 describes the number of cases notified by each commune.

219 **Spatial autocorrelation**

220 Table 1 shows the Global Moran's I statistics for each individual year within our study period. We
221 observed clear but weak spatial autocorrelation in TB notified incidence throughout the study period.
222 While the Moran's I values were modest, the autocorrelation appeared to weaken in later years.

223 **Bayesian spatio-temporal modelling**

224 Table 2 presents a comparison of the candidate models' goodness-of-fit metrics, including those
225 incorporating the effective number of parameters. Though Models 4a and 4b were both potential
226 candidates based on their DIC and WAIC values, Model 4b was our preferred choice for further
227 analysis owing to its lower DIC. Models 2a and 2b also demonstrated relatively strong performance,
228 with moderate DIC and WAIC values. Model 5b had the lowest posterior mean deviance but also the
229 highest effective number of parameters, resulting in the highest DIC. Model M4b had the additional
230 advantage of permitting estimation of the effects of areal covariates.

231 Table 3 presents the fixed effects of poor households and population density on TB SMRs using
232 Model 4b. The proportion of poor households was significantly and positively correlated with TB
233 SMRs. The distribution for the coefficient for poor household proportion indicated that each
234 percentage point increase in the proportion of poor households of a commune was associated with a
235 1.3% (95% CrI: 0.1% - 2.5%) increase in predicted TB notifications. On the other hand, population
236 density did not appear to be associated with TB SMR. The mean and median estimation for the
237 distribution of the coefficient was 0.001, indicating a 0.1% rise in TB notifications for each 1000
238 people/km² change in population density. However, the 95% CrI (-0.009 - 0.01) indicates that it is
239 plausible that population density had no association with TB notifications. Figure S4 (Supplementary
240 Material) displays the marginal posterior distribution of the proportion of poor households, which
241 represents the probability distribution of this parameter after accounting for the effects of all other
242 parameters in the model. Figure 3 presents the model predicted TB relative risks of 226 communes
243 over the study period.

244

245

246 **Sensitivity analysis**

247 The choice of hyperpriors impacted the model's performance, as reflected in differences in the
248 effective number of parameters across prior choices (Table 4). Despite this, the estimates for key
249 covariates remained qualitatively robust. For example, the fixed effect of poor household proportions
250 showed minimal variations in posterior means and medians, with overlapping 95% CrIs across all
251 prior configurations. Similarly, the fixed effect of population density demonstrated small changes, with
252 consistent interpretations of the estimates.

253 Table S2 presents the goodness-of-fit comparison for models with a negative binomial distribution for
254 TB notifications. Model 4b consistently exhibited the lowest DIC, achieving the best balance between
255 fit and complexity of the models considered.

256

257 **DISCUSSION**

258 We analysed commune-level adult TB notification counts in Nam Dinh Province, Vietnam,
259 from 2013 to 2022 at the smallest administrative level. Significant clustering was observed across 226
260 communes through spatial autocorrelation for most of the ten-year study period. Among twelve
261 candidate Bayesian disease mapping models, those incorporating spatial and temporal effects along
262 with unstructured interactions achieved the best balance between goodness-of-fit and complexity.
263 During this period, 14,887 TB cases were recorded, with the notification rate peaking at approximately
264 100 cases per 100,000 population in 2017 and falling to a low of about 60 cases per 100,000 in 2021.
265 A likely contributor to the decline in TB notifications in 2021 was the COVID-19 pandemic, which
266 disrupted TB control efforts through limited healthcare access, resource reallocation and changes in
267 social behaviours that may have impacted transmission patterns [23,24].

268 Overall, models that incorporated different types of space-time interactions (Models 4a to 6b)
269 outperformed those with only spatial main effects (Model 1a and Model 1b), spatial unstructured
270 effects and temporal effects (Model 2a and Model 2b), or a combination of spatial and temporal main
271 effects (Model 3a and Model 3b). Among the models incorporating space-time interactions, Model 5b,
272 which allowed for unstructured spatial and structured temporal effects with covariates, showed
273 potential in capturing local dynamics and achieved the lowest posterior mean deviance. However, this
274 model also exhibited a higher effective number of parameters, likely due to the complex temporal
275 structure of the data. For example, some communes showed recent spikes in TB transmission with

276 consistent increases in notifications, while others exhibited stable or declining trends. This variation
277 could be attributable to the impact of recent transmission (as opposed to reactivation of latent TB
278 infection), given the potentially long duration from infection to active disease. However, this
279 interpretation is not conclusive because this approach did not achieve the best overall performance.
280 Notably, models incorporating spatial effects, temporal effects, and the interaction of unstructured
281 spatial with temporal effects (Model 4a and Model 4b) showed the optimal balance between
282 goodness-of-fit and complexity based on DIC values. This suggests that the spatial and temporal
283 trends of TB may be influenced by neighbouring areas in the short term, with local outbreaks
284 potentially spreading across adjacent regions, since only a small proportion of TB cases are likely to
285 result from transmission between household members and known social contacts [25].
286 Incorporating the proportion of poor households and population density as covariates into Model 4b
287 and 5b lowered the deviance. Although not a definitive finding, these results are consistent with other
288 research that has found that social factors can contribute to variation in TB rates, particularly
289 indicators of socioeconomic disadvantages [19,26].
290 Our findings might have some limitations. First, the results may be sensitive to the modifiable area
291 unit problem, which arises in spatial analysis when the results of a study are influenced by the choice
292 of spatial units or boundaries used to aggregate the data [27]. *M.tb* transmission frequently occurs at
293 the household level [28], leading to highly localized outbreaks. Our areal units, such as communes,
294 may smooth over numerous individual epidemics occurring simultaneously within different households
295 or communities. However, *M.tb* can also spread across large distances due to human mobility, driven
296 by its prolonged disease duration and extended latency period [28]. This combination of very local
297 transmission and long-range spread introduces unique challenges for spatial analysis of TB. Second,
298 our analysis is based on commune-level data from the electronic system of the NTP, which, while
299 being the best available data source, may be subject to reporting inaccuracies, incomplete case
300 capture, or delays in notification. Such issues could introduce biases into the spatial patterns and
301 temporal trends observed in our study. Additionally, this data may lack granularity on socioeconomic
302 variables, comorbidities, or healthcare access, which could provide a more comprehensive
303 understanding of the factors driving *M.tb* transmission.
304 Our systematic approach to model selection considered space, time, their interaction and
305 socioeconomic factors over a significant period. By employing techniques such as spatial

306 autocorrelation analysis, exploratory data visualization, and advanced Bayesian models, we
307 uncovered TB patterns and trends that are not immediately apparent when only considering case
308 counts in each area. By identifying communes with TB spikes or high-risk areas - such as those with
309 elevated TB risk or higher poverty levels - resources can be allocated more effectively, prioritizing TB
310 active case finding (ACF) activities in those areas. Studies have shown that combining spatial
311 analysis with ACF can significantly increase TB detection in these areas [29]. However, this
312 consideration must be balanced against the efficiency of applying policies and programs consistently
313 across the country or individual provinces, which may be more efficient given the unpredictable nature
314 of the epidemic. Additionally, integrating local socioeconomic data - such as income levels, education,
315 population density, and healthcare access - into the TB surveillance system and applying Bayesian
316 spatio-temporal analysis methods across broader regions could enhance predictive capabilities.

317

318 **CONCLUSIONS:**

319 We conducted an analysis of TB notifications in Nam Dinh Province from 2013 to 2022, finding clear
320 but weak spatial autocorrelation across 226 communes over most of the ten-year period. Among the
321 Bayesian methods evaluated, the model that incorporated spatial effects, temporal effect and
322 unstructured interactions struck the best balance between complexity and goodness-of-fit. A more
323 highly parameterised model with structured temporal and unstructured spatial interactions potentially
324 offered the best fit to the evolving patterns of the data, suggesting that individual communes may
325 exhibit distinct trends. Identifying consistent patterns without overfitting is challenging, likely due to the
326 epidemic's complexity and interacting epidemiological factors that include recent transmission, case
327 detection, and past infection reactivation. The incorporation of socioeconomic indicators provided
328 deeper insights into TB patterns, with the proportion of poor households identified as a likely
329 influencing factor. This approach can be adapted to enhance TB management in Vietnam and other
330 regions. Integrating areal socioeconomic data and other covariates with Bayesian spatio-temporal
331 analysis across broader regions could enhance our understanding of TB epidemiology, while
332 collecting additional individual-level data through enhanced surveillance would be even more
333 beneficial.

334

335

336 **DECLARATIONS**

337 **Ethics approval and consent to participate:** Ethics approval for this study was granted by the
338 Human Ethics Low Risk Review Committee at Monash University, under project number 41463, on
339 February 7, 2024.

340 **Availability of data and materials:** The dataset includes sensitive individual information and cannot
341 be publicly shared. Interested researchers should contact Dr. Nguyen Binh Hoa at
342 nguyenbinhhoatb@yahoo.com. The code used for analysis is available on GitHub at
343 github.com/longbui189/SPTB-VN.

344 **Competing interests:** The authors declare that they have no competing interests.

345 **Author Contributions**

346 **Viet Long Bui:** Conceptualization, Methodology, Data Curation, Software, Writing- Original draft
347 preparation; Writing- Reviewing and Editing; **Romain Ragonnet:** Conceptualization, Methodology,
348 Writing- Reviewing and Editing; **Angus Hughes:** Conceptualization, Methodology, Writing- Reviewing
349 and Editing, **Hoa Nguyen Binh:** Data Curation, Writing- Reviewing and Editing; **Nam Do Hoang:**
350 Data Curation, Software; **Emma S. McBryde:** Writing- Reviewing and Editing; **Justin Sexton:**
351 Writing- Reviewing and Editing, Methodology; **Thuy Phuong Nguyen:** Writing- Reviewing and
352 Editing; **David Shipman:** Software; **Greg J. Fox:** Conceptualization, Data Curation, Methodology,
353 Writing- Reviewing and Editing; **James M. Trauer:** Conceptualization, Methodology, Data Curation,
354 Software, Writing- Reviewing and Editing, Supervision.

355 **Acknowledgements:** Viet Long Bui received a full postgraduate scholarship from Monash University,
356 awarded to facilitate the research presented in this study. James M. Trauer is a recipient of a
357 Discovery Early Career Fellowship from the Australian Research Council (DE230100730). The
358 funders had no role in study design, data collection and analysis, decision to publish, or preparation of
359 the manuscript.

360

361

362

363 REFERENCES

- 364 1. Villar-Hernández R, et al. Tuberculosis: current challenges and beyond. *Breathe* 2023; **19**:
365 220166.
- 366 2. World Health Organization. *Global tuberculosis report 2023*. World Health Organization,
367 2023.
- 368 3. Lönnroth K, et al. Drivers of tuberculosis epidemics: the role of risk factors and social
369 determinants. *Social Science & Medicine (1982)* 2009; **68**: 2240–2246.
- 370 4. Moonan PK, et al. Does directly observed therapy (DOT) reduce drug resistant tuberculosis?
371 *BMC Public Health* 2011; **11**: 19.
- 372 5. Theron G, et al. Data for action: collection and use of local data to end tuberculosis. *The*
373 *Lancet Elsevier*, 2015; **386**: 2324–2333.
- 374 6. van Gorp M, et al. Finding gaps in TB notifications: spatial analysis of geographical patterns
375 of TB notifications, associations with TB program efforts and social determinants of TB risk in
376 Bangladesh, Nepal and Pakistan. *BMC Infectious Diseases* 2020; **20**: 490.
- 377 7. Shaweno D, et al. Methods used in the spatial analysis of tuberculosis epidemiology: a
378 systematic review. *BMC Medicine* 2018; **16**: 193.
- 379 8. Besag J, York J, Mollié A. Bayesian image restoration, with two applications in spatial
380 statistics. *Annals of the Institute of Statistical Mathematics* 1991; **43**: 1–20.
- 381 9. Riebler A, et al. An intuitive Bayesian spatial model for disease mapping that accounts for
382 scaling. *Statistical Methods in Medical Research* SAGE Publications Ltd STM, 2016; **25**: 1145–1165.
- 383 10. Knorr-Held L. Bayesian modelling of inseparable space-time variation in disease risk.
384 *Statistics in Medicine* 2000; **19**: 2555–2567.
- 385 11. Blangiardo M, et al. Spatial and spatio-temporal models with R-INLA. *Spatial and Spatio-*
386 *temporal Epidemiology* 2013; **4**: 33–49.
- 387 12. GADM. (<https://gadm.org/maps/VNM.html>). Accessed 4 April 2024.
- 388 13. Acosta LA Grant Morrison, Angela Li, Karina. *Chapter 6 Contiguity-Based Spatial Weights*
389 *| Hands-On Spatial Data Science with R*.
- 390 14. Moran PAP. Notes on Continuous Stochastic Phenomena. *Biometrika* [Oxford University
391 Press, Biometrika Trust], 1950; **37**: 17–23.
- 392 15. Lawson AB. *Using R for Bayesian Spatial and Spatio-Temporal Health Modeling*. CRC
393 Press, 2021.
- 394 16. Bernardinelli L, Clayton D, Montomoli C. Bayesian estimates of disease maps: How
395 important are priors? *Statistics in Medicine* 1995; **14**: 2411–2431.
- 396 17. Rue H, Martino S, Chopin N. Approximate Bayesian inference for latent Gaussian models by
397 using integrated nested Laplace approximations. *Journal of the Royal Statistical Society: Series B*
398 *(Statistical Methodology)* 2009; **71**: 319–392.
- 399 18. Thanh Binh PT, Ha VV. Poverty Reduction in Vietnam and the Role of Public Administration.
400 *Journal of Contemporary Asia* Routledge, 2019; **49**: 151–163.
- 401 19. Duarte R, et al. Tuberculosis, social determinants and co-morbidities (including HIV).
402 *Pulmonology* 2018; **24**: 115–119.
- 403 20. Spiegelhalter DJ, et al. Bayesian measures of model complexity and fit. *Journal of the Royal*
404 *Statistical Society: Series B (Statistical Methodology)* 2002; **64**: 583–639.

- 405 21. **Watanabe S.** A widely applicable Bayesian information criterion. *The Journal of Machine*
406 *Learning Research* 2013; **14**: 867–897.
- 407 22. **R Core Team.** *R: a language and environment for statistical computing*. Vienna, Austria: R
408 Foundation for Statistical Computing, 2022.
- 409 23. **McQuaid CF, et al.** The impact of COVID-19 on TB: a review of the data. *The International*
410 *Journal of Tuberculosis and Lung Disease* 2021; **25**: 436–446.
- 411 24. **Kessel B, et al.** Impact of COVID-19 pandemic and anti-pandemic measures on tuberculosis,
412 viral hepatitis, HIV/AIDS and malaria—A systematic review. *PLOS Global Public Health* Public Library
413 of Science, 2023; **3**: e0001018.
- 414 25. **McCreesh N, White RG.** An explanation for the low proportion of tuberculosis that results
415 from transmission between household and known social contacts. *Sci Rep* 2018; **8**: 5382.
- 416 26. **Siroka A, et al.** The effect of household poverty on tuberculosis. *The international journal of*
417 *tuberculosis and lung disease : the official journal of the International Union against Tuberculosis and*
418 *Lung Disease* 2016; **20**: 1603–1608.
- 419 27. **Buzzelli M.** Modifiable Areal Unit Problem. *International Encyclopedia of Human Geography*
420 2020; : 169–173.
- 421 28. **Coleman M, et al.** Mycobacterium tuberculosis transmission in high-incidence settings—new
422 paradigms and insights. *Pathogens (Basel, Switzerland)* 2022; **11**Published online:
423 2022.doi:10.3390/pathogens11111228.
- 424 29. **Robsky KO, et al.** Spatial distribution of people diagnosed with tuberculosis through routine
425 and active case finding: a community-based study in Kampala, Uganda. *Infectious Diseases of*
426 *Poverty* 2020; **9**: 73.
- 427
- 428
- 429

430 **Table 1. Global Moran's I statistics**

Year	Moran's I	p value
2013	0.094	<0.01**
2014	0.117	<0.01**
2015	0.081	0.02*
2016	0.091	0.01*
2017	0.071	<0.01**
2018	0.060	0.06*
2019	0.129	<0.01**
2020	0.069	0.04*
2021	0.043	0.12
2022	0.051	0.08

431 *Moran's I expected value: 0.444. * p < 0.05, ** p < 0.01.*

432

Accepted Manuscript

433 **Table 2. Goodness of fit comparison of models**

Model	\bar{D}	ρ_D	DIC	Δ_{DIC}	WAIC	Δ_{WAIC}
Model 1a	10507.05	165.26	10672.31	27.63	10696.48	35.58
Model 1b	10506.42	166.19	10672.61	27.93	10697.56	36.66
Model 2a	10517.63	158.34	10675.97	31.29	10698.42	37.52
Model 2b	10517.57	159.50	10677.07	32.29	10700.63	39.73
Model 3a	10508.15	167.18	10675.33	30.65	10700.48	39.58
Model 3b	10506.71	167.96	10674.67	29.99	10700.19	39.29
Model 4a	10264.22	382.31	10646.53	1.85	10660.50	-0.40
Model 4b	10264.66	380.06	10644.68	Referent	10660.90	Referent
Model 5a	10292.21	511.07	10803.28	158.60	10808.15	147.25
Model 5b	10235.32	601.75	10837.07	192.39	10820.21	159.31
Model 6a	10354.35	290.04	10644.38	-0.30	10667.24	6.34
Model 6b	10375.62	273.49	10649.11	4.43	10673.56	12.66

434 \bar{D} : Posterior mean deviance, ρ_D : Effective numbers of parameters, DIC: Deviance Information

435 Criterion, Δ_{DIC} , Δ_{WAIC} Difference in DIC and WAIC relative to Model 4b, respectively. Our preferred

436 model (Model 4b) was used as the referent analysis for comparison of information criteria.

437

Accepted

438 **Table 3: Fixed effects of the Model 4b**

Fixed effect variable	Mean (SD)	Median (95% CrI)
Poor household proportion	0.013 (0.005)	0.013 (0.001 – 0.025)
Population density	0.001 (0.005)	0.001 (-0.009 – 0.01)

439 *SD: standard deviation, 95% CrI: 0.025 quantile - 97.5 quantile*

440

441

Accepted Manuscript

442 **Table 4: Sensitivity analysis results of the Model 4b**

	Log-gamma prior		
	shape = 1	shape = 0.01	shape = 2
	rate = 0.0005	rate = 0.01	rate = 0.5
Fixed effect of poor household proportion			
Mean (SD)	0.013 (0.005)	0.012 (0.007)	0.014 (0.007)
Median	0.013	0.013	0.012
(95% CrI)	(0.001 - 0.025)	(0.001 - 0.025)	(0.001 - 0.025)
Fixed effect of population density			
Mean (SD)	0.001 (0.005)	0.001 (0.005)	-0.002 (0.005)
Median	0.001	0.001	-0.002
(95% CrI)	(-0.009 - 0.01)	(-0.009 - 0.01)	(-0.011 - 0.002)

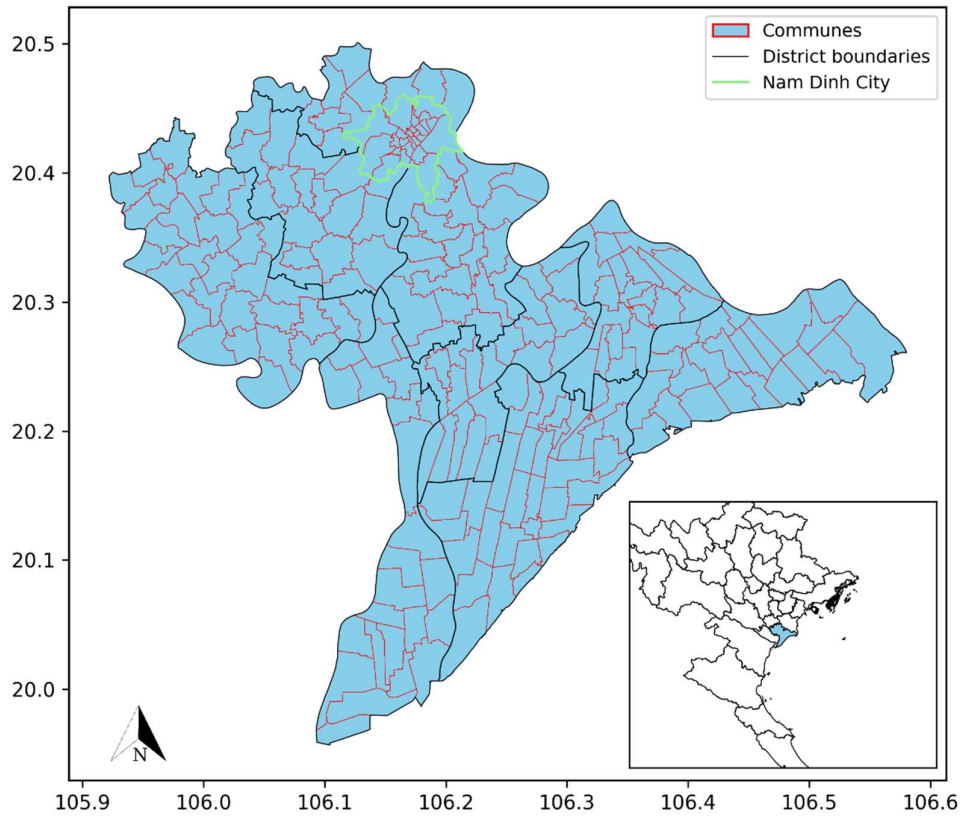
443 ρ_D : Effective numbers of parameters. SD: standard deviation, 95% CrI: 0.025 quantile - 97.5 quantile

444

Accepted Manuscript

445 **Figure 1. Base map of Nam Dinh Province.** *World Geodetic System 84 Universal Transverse*

446 *Mercator Zone 48N.*

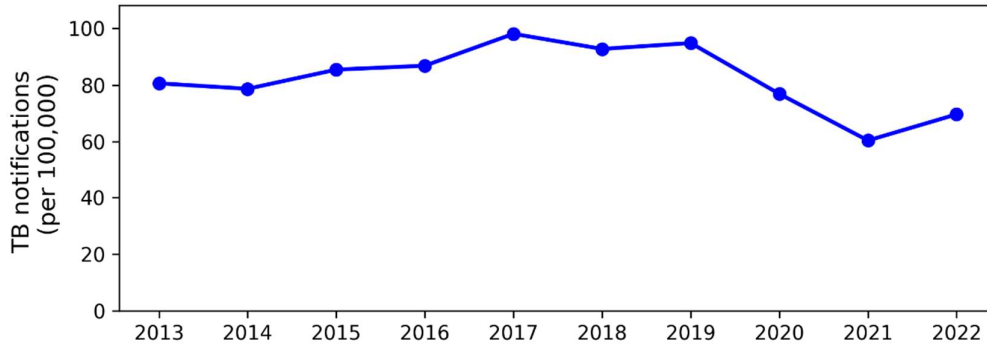


447

448

ACC

449 **Figure 2. TB notifications per 100,000 population in Nam Dinh Province by study year.**

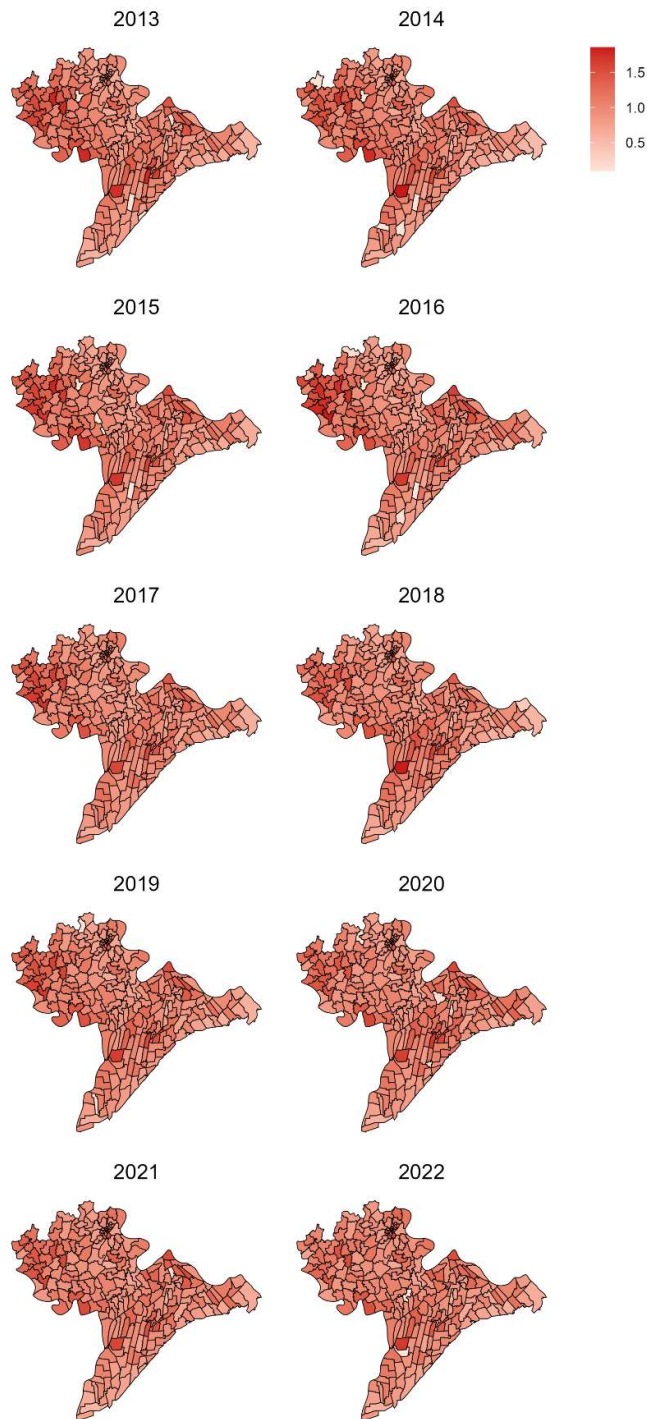


450

451

Accepted Manuscript

452 **Figure 3. Predicted TB relative risks in Nam Dinh Province, from 2013 to 2022.**



453